Supporting Information

Electroactive Edge Site-Enriched Nickel-Cobalt Sulfide into Graphene Frameworks for High-performance Asymmetric Supercapacitors

Juan Yang, Chang Yu, Xiaoming Fan, Suxia Liang, Shaofeng Li, Huawei Huang, Zheng Ling, Hao Ce, and Jieshan Qiu*

Theoretical calculations

Computational Models: The model of spinel Ni-Co-S species was constructed, in which the Co atoms in Co_3S_4 were partially replaced by Ni atoms, e.g. $Ni_{1.5}Co_{1.5}S_4$ (Figure S13) and the same amount of Ni and Co atoms in one unit cell and the same spinel structure (Fd3m) as Co_3S_4 were adopted.

The Ni-Co-S (311) and (220) surfaces including four and three atomic layers, respectively, were modeled as a p (1×1) periodic slab. The atoms in the top two layers were relaxed, and all other atoms were fully frozen. The neighboring layers were separated in the direction perpendicular to the surface by a vacuum distance of 15 Å.

Computational Methods: The spin-polarized DFT calculations were performed using projector augmented wave (PAW) potentials and the Perdew-Burke-Ernzarhof (PBE) functional implemented in the *Vienna ab initio* simulation package (VASP). [1-4] Relaxations were carried out using conjugate-gradient algorithm. The occupancy of the one-electron states was calculated using the Gaussian smearing (SIGMA = 0.1 eV). The energy convergence was selected 1×10^{-4} eV atom^{-1}. The kinetic-energy cutoff of plane wave was set to 400 eV. The Brillouin-zone was integrated using Monkhorst-Pack-generated sets of k points. A 5×5×5 and 2×2×1 k-points grid was used for the bulk and surface calculation, respectively. The surface energy (E_{surf}) can be calculated as follows:

$$E_{surf} = (E^{n}_{slab} + nE_{bulk}) / 2A$$

where E^{n}_{slab} is the total energy of the slab, E_{bulk} is the total energy of the bulk per unit cell, n is the number of bulk unit cells contained in the slab, and A is the surface area of each side for the slab.

The adsorption energy (E_{OH^-}) of hydroxide ion (OH^-) in electrolyte on the metal atoms of Ni-Co-S (311) and (220) surfaces was investigated, in which a corresponding 1×1×1 k points mesh was used during optimizations after a 2×2×1 mesh pre-checking tests. The E_{OH-} was defined as the total energys difference between desorption and adsorption of OH^- on the two surfaces.

[1] G. Kresse, & J. Hafner, *Phys. Rev. B*, **1994**, 49, 14251.

[2] G. Kresse, & J.Furthmuller, *Comput. Mater. Sci.*, **1996**, 6, 15.

[3] G. Kresse, & J. Furthmuller, *Phys. Rev. B*, **1996**, 54, 11169.

[4] P. E.Blöchl, *Phys. Rev. B*, **1994**, 50, 17953.

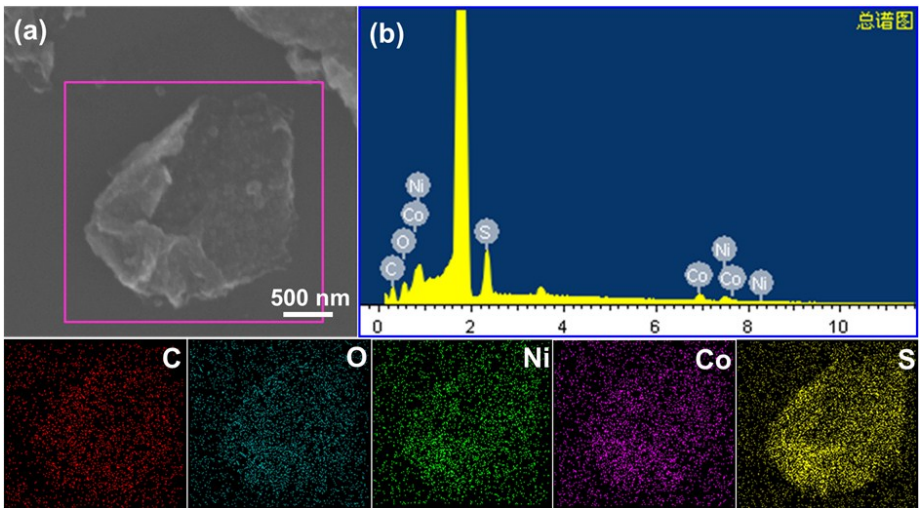

Figure S1. SEM image and its EDS spectrum of the integrated edge site-enriched Ni-Co-S/G hybrids on silicon substrate, as well as corresponding elemental mapping from the square region marked in (a), demonstrating that it is made of Co, Ni, S, C, and O species. The O species is mainly attributed to some oxygen-containing functional groups on graphene surface, which is consistent with C1s XPS spectrum result. Moreover, these functional groups could effectively enhance the structural stability of electrode materials and improve their wettability, and further deliver the excellent electrochemical performance.

Table S1 The relative contents of elements in Ni-Co-S/G hybrids derived from EDS data.

Element	Ni	Co	S
wt%	8.81	8.22	12.45
at%	2.46	2.32	6.45

From Table S1, it can be noted that the molar ratio of Ni, Co and S is *ca.* 1:1: 2.69. In the case, the x value for $Ni_xCo_{3-x}S_4$ is calculated, *ca.* 1.5. In other words, about a half amount of Co atoms in the Co_3S_4 is substituted by Ni atoms.

Table S2 The Ni and Co contents in Ni-Co-S/G hybrids based on ICP data.

Element	Ni	Co
wt%	8.96	8.97

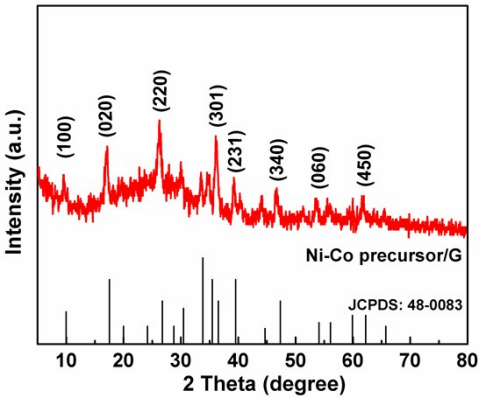

Figure S2. Typical XRD patterns of the Ni-Co precursor/G hybrids and NiCo-carbonate hydroxides (JCPDS Card no. 48-0083).

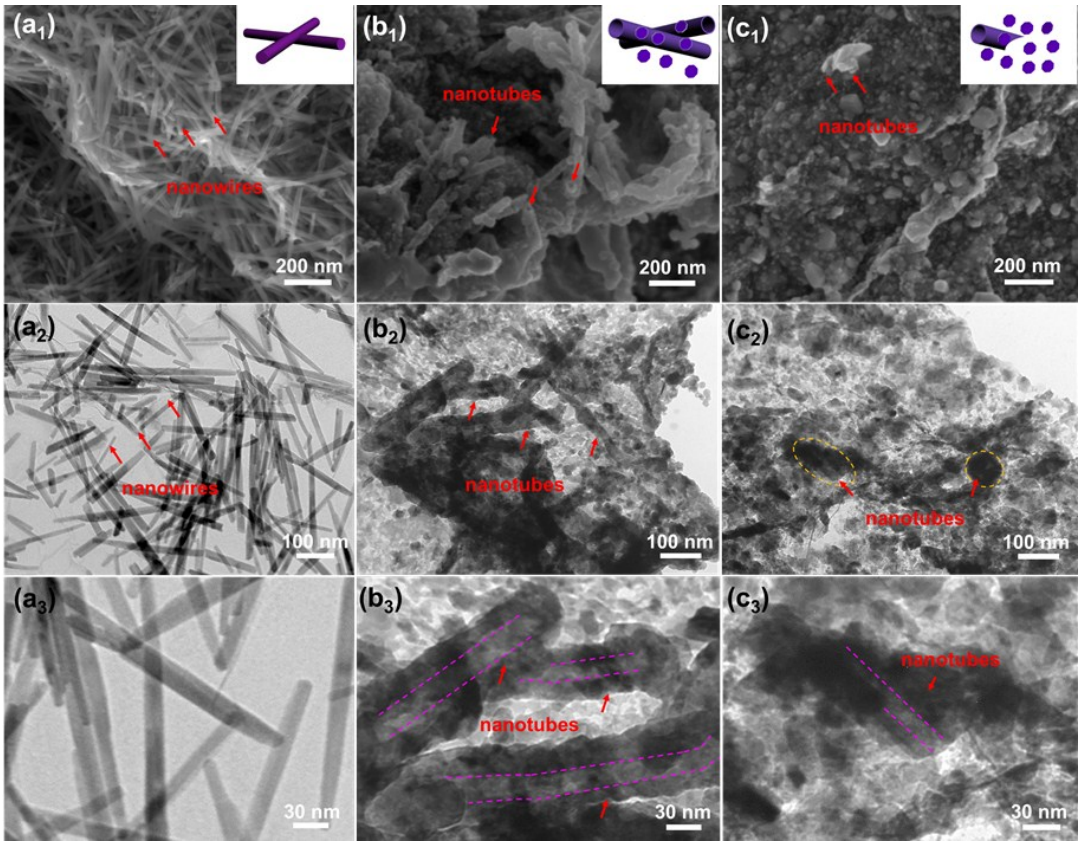

Figure S3. Typical FE-SEM and TEM images of the as-abtained Ni-Co precursor/G in the presence of TAA at different reaction stages: (a_1, a_2, a_3) 0 h, (b_1, b_2, b_3) 3 h, and (c_1, c_2, c_3) 6 h.

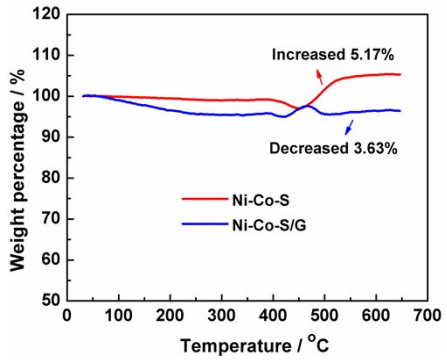

Figure S4. TGA curves of the pristine Ni-Co-S in the absence of G and Ni-Co-S/G hybrid samples under air, demonstrating that the weight fraction of Ni-Co-S in integrated Ni-Co-S/G hybrids is *ca.* 91.7% according to the mass increase and loss of samples.

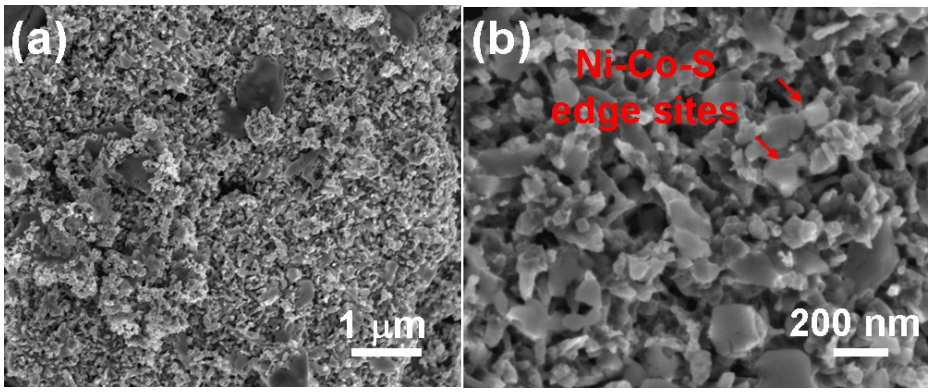

Figure S5. Typical FE-SEM images of the pristine Ni-Co-S nanoparticles in the absence of graphene.

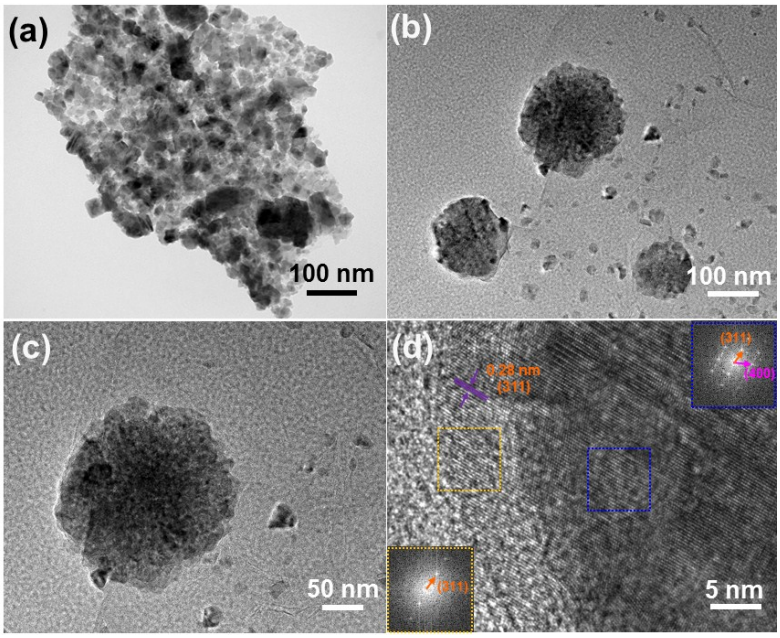

Figure S6. (a) TEM images of the integrated edge site-enriched Ni-Co-S/G hybrids, (b, c) TEM and (d) HR-TEM images of the B-Ni-Co-S/G hybrids, the inset is FFT images obtained from the square region.

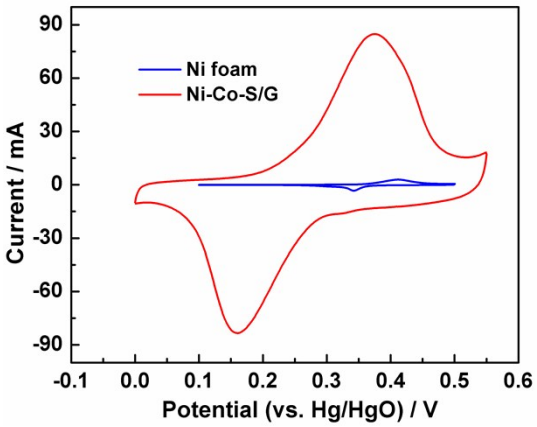

Figure S7. CV curves of the nickel foam and integrated edge site-enriched Ni-Co-S/G hybrid electrodes at a constant scan rate of 10 mV s^{-1}.

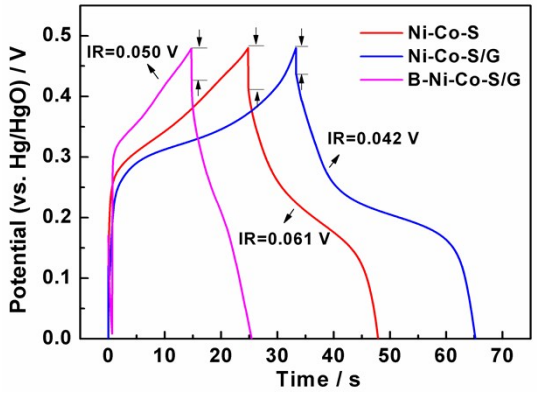

Figure S8. Galvanostatic charge/discharge curves of the pristine Ni-Co-S, integrated edge site-enriched Ni-Co-S/G, and B-Ni-Co-S/G hybrids at current density of 20 A g^{-1}.

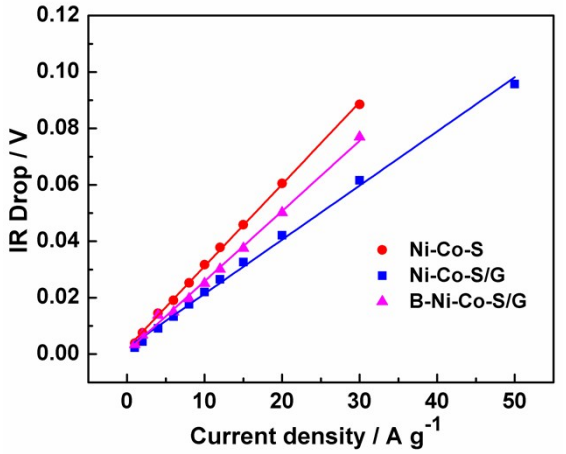

Figure S9. Potential drop (IR drop) of the pristine Ni-Co-S in the absence of G, integrated edge site-enriched Ni-Co-S/G, and B-Ni-Co-S/G hybrid electrodes at different discharge current densities.

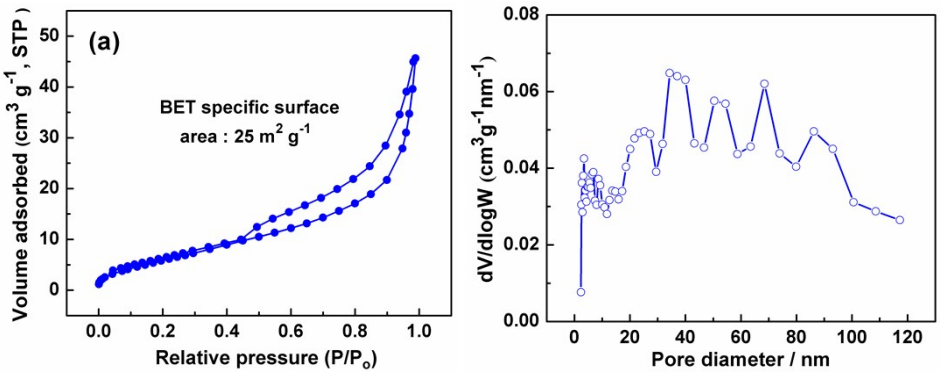

Figure S10. Nitrogen adsorption/desorption isotherms (a) and the corresponding pore size distribution (b) of the integrated edge site-enriched Ni-Co-S/G samples.

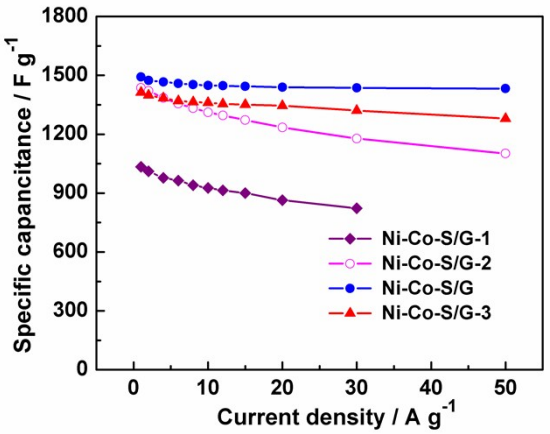

Figure S11. The specific capacitances of the as-made Ni-Co-S/G-1, Ni-Co-S/G-2, Ni-Co-S/G, Ni-Co-S/G-3 hybrids at different current densities.

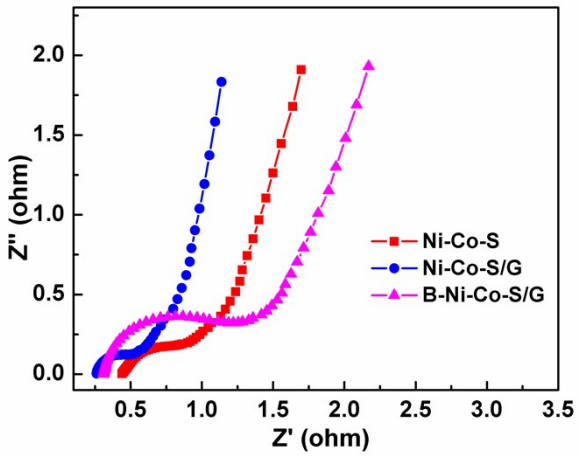

Figure S12. Nyquist plots of electrochemical impedance spectroscopy (EIS) data for the Ni-Co-S, integrated edge site-enriched Ni-Co-S/G hybrids, and directly fabricated B-Ni-Co-S/G hybrids.

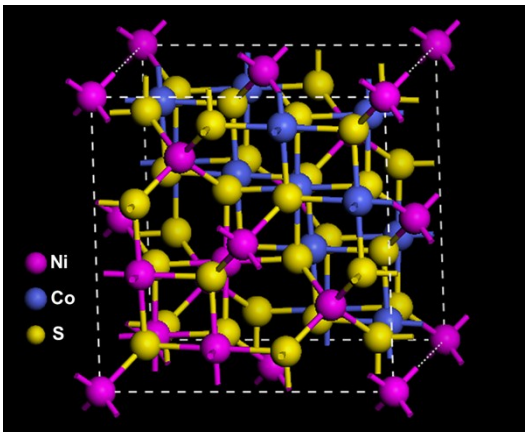

Figure S13. DFT structure models of Ni-Co-S, in which a half amount of the Co atoms in the spinel Co_3S_4 was replaced by Ni atoms, e.g. $Ni_{1.5}Co_{1.5}S_4$.

Table S3 The evaluated surface energies (E_{surf}) of the Ni-Co-S (311) and (220) plane surfaces.

Ni-Co-S plane surfaces	(311)	(220)
E_{surf} / J m^{-2}	1.278	0.457

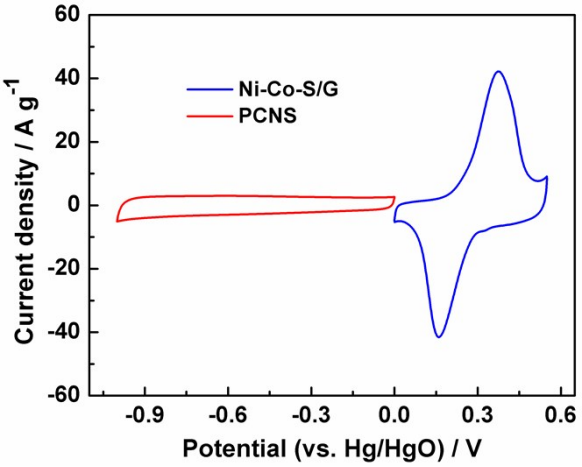

Figure S14. CV curves of the PCNS and integrated edge site-enriched Ni-Co-S/G hybrid electrodes at a constant scan rate of 10 mV s^{-1}.